

Enhanced Dynamic Droop Control for Microgrid Frequency and Voltage Stabilization Using Hybrid Energy Storage Systems: A SECANT Method Approach

Sunday Oladejo Adetona  , Kenneth Ugo Udeze  *

Department of Electrical and Electronics Engineering, University of Lagos, Lagos, Nigeria.

ABSTRACT

Due to their variable and intermittent nature, the integration of renewable energy sources poses control challenges related to voltage and frequency stability in isolated microgrids. This paper proposes an enhanced dynamic droop control strategy optimized in active time along with a Hybrid Energy Storage System (HESS) comprising Battery Energy Storage System (BESS), supercapacitors (SUPCA), and Superconducting Magnetic Energy Storage (SMES) to improve microgrid stability. The Dynamic Droop Gains (DDG) are continuously tuned using the rapid-converging SECANT numerical method to enhance transient response and steady-state performance, this was achieved using MATLAB/Simulink. The HESS combines the complementary characteristics of BESS, SUPCA and SMES to balance steady power supply and temporary overload capacity. Detailed simulation studies on a microgrid test system verify that the proposed control strategy significantly enhances voltage/frequency regulation, power sharing accuracy, BESS lifespan and overall stability compared to conventional droop techniques. The SUPCA further improves the transient performance and power quality by mitigating fluctuations. The research demonstrates an innovative way to harness advanced control algorithms and emerging storage technologies for next-generation resilient and sustainable microgrids.

Keywords: Microgrid, Energy storage systems, Battery energy storage, Superconducting magnetic energy storage, Super-capacitors.

1. INTRODUCTION

Small-scale energy distribution systems also known as microgrids (MGs) can provide a localized area with continuous electricity (Li et al., 2017). The concept of MGs has raised a lot of interest in recent times as a feasible way to improve the efficiency and pliability of power distribution networks (Fu et al., 2015; Ibrahim et al., 2017). Their capacity to lower greenhouse gas emissions and carbon emissions while improving power system flexibility mostly in the event of disruptions or outages is what is driving the increasing interest

*Corresponding author

Peer review under the responsibility of University of Baghdad.

<https://doi.org/10.31026/j.eng.2024.09.01>

This is an open access article under the CC BY 4 license (<http://creativecommons.org/licenses/by/4.0/>).

Article received: 09/05/2024

Article revised: 23/08/2024

Article accepted: 28/08/2024

Article published: 01/09/2024



(Oguntosin and Ogbechie, 2023). Their capacity to function either independently or in collaboration with a central power grid distinguishes them and provides a dynamic and decentralized method of energy production and distribution **(Serban and Marinescu, 2014)**.

Synchronous generators, wind turbines, and photovoltaic (PV) systems are examples of Distributed Energy Resources (DERs) that can be included into a MG. Local electric power generation is made possible by these DERs taken together **(Marzebali et al., 2020; Saeed et al., 2021)**. Storage of energy is indispensable in MGs; in that, it gives room for excess energy produced in time of surplus generation to be stored, and then released in time of crest power demand **(Aghamohammadi and Abdolahinia, 2014; Oguntosin and Ogbechie, 2023)**. The Hybrid Energy Storage System (HESS); which includes Battery Energy Storage System (BESS), Superconducting Magnetic Energy Storage (SMES), and Super-capacitors (SUPCA) has been looked into in MG research; so as to extend the life of BESS, lower outlays, and ameliorate overall efficiency of the MGs **(Hajiaghasi et al., 2019)**.

In MGs, the consolidation of HESS is very crucial; because it puts up massively to the effective use of renewable energy sources, stability of the grids, and reduces dependence on fossil fuels **(Marzebali et al., 2020)**. Notwithstanding, the high penetration of DERs in MGs has several issues and problems associated with frequency and voltage stability because of their unpredictable attributes.

Formal methods of droop control are already being utilized for sharing and allocating loads among DERs in MGs. All the same, they experience problems such as load-sharing issues, erratic sharing, and unstableness under some stipulations **(Li et al., 2017)**. Several enhanced techniques for droop control are already proposed to resolve these problems using techniques such as adaptive and dynamic droop gains, simulated impedances, organised control loops etc.

An organised control technique for battery-super-capacitor HESS in a complete Alternating Current MG was proposed in **(Ren et al., 2020)**. SUPCA resolves the issues concerning high-frequency fluctuation of power, while BESS resolves issues concerning low-frequency parts; thereby bringing down the tension on BESS and also prolonging lifespan of BESS. Adaptive droop control techniques showed better load sharing capabilities compared to traditional droop control methods. The model was validated with PSCAD/EMTDC software, and simulation was conducted to test the operation performance of the HESS under disturbance. In another study by **(Lin and Lei, 2017)**, an organised control technique for HESS which comprises of SMES and BESS was proposed. The technique was targeted at enhancing performance of HESS and to attain efficient connection for wind farm. The model was established on Proportional-Integral (PI) and Energy Shaping (ES) controls using port-controlled Hamiltonian model. The results of this simulation showed that the ES control showed better robustness compared to conventional PI control and massively reduces the issues of parameter tuning. A control method for standalone MGs with high unpredictable renewable generation system penetration was presented by **(Kim et al., 2016)**. This technique comprises of BESS used to generate nominal frequency and make the system frequency independent of a synchronous generator's mechanical inertia. Diesel Generator (DG) was used to maintain State of Charge (SOC) of the BESS at a certain value, and Q/P droop control was introduced to the renewable system to check fluctuations of generated voltage. This technique was simulated, and the results revealed that the technique effectively resolved the issues presented by unpredictable power output. The model for this system was



based on data from the Ulleungdo power plant, and it was modeled and simulated in the MATLAB environment.

The study conducted by **(Opiyo, 2018)** exhibited droop control techniques for PV-based mini-grids with different line impedances. The model comprises of PV-array, BESS, and load. The following droop control techniques were studied; active power-frequency and reactive power-voltage. The results revealed that active power frequency control is more effective for low X/R ratio, while reactive power voltage is better for high X/R ratios. It was also noted in the study that a shunt-connected inverter controlled the power flow in the grid effectively. The study conducted by **(Li et al., 2017)** developed and tested HESS for main frequency control in a detached MG power plant. The study proposed a dynamic droop control technique for HESS; and compared its performance with the preceding control technique. The proposed model was simulated in the PSCAD/EMTDC environment with the MG and SMES/BESS/HESS. The simulated results revealed that the dynamic droop control technique substantially improved the frequency regulation features of HESS and also prolonged the usable lifetime of the BESS part.

Lately, **(Marzebali et al., 2020)** developed an adaptive droop-based control technique for fuel cell-battery HESS; for holding up primary frequency for stand-alone MGs. In the study, the system comprises of wind turbine (WT), Photovoltaic (PV) system, fuel-cell, BESS, and a suited system for supervising energy. The technique allowed power sharing between fuel cell and BESS using a droop controller in upholding primary frequency in a preset guarantee range. The simulated results disclosed that the proposed technique stabilized the voltage and frequency of MG effectively. This shows that dynamic droop control technique that occasionally updates droop gains has promising enhancement performance among more advanced techniques for system control. But optimally tuning the droop gains in active-time is complex. Therefore, this current study proposes a new technique by combining dynamic droop control and HESS to improve stability of MG. Dynamic Droop Gains (DDGs) were optimized using SECANT technique because it provides fast convergence for occasional on-line gain tuning. The BESS and SUPCA are incorporated as an HESS in order to synergize their attributes; and also to sustain the MG during disturbances.

Detailed simulations are presented to demonstrate the effectiveness of this proposed technique compared to the usual droop control. The results exhibited substantially enhanced stability under different load conditions. The HESS handled fluctuations of power effortlessly while dynamic droop control ensured optimal system response. This study offers forward-thinking direction towards advanced control methods and BESS for next-generation MGs.

2. MATERIAL AND METHODS

An MG is formulated to enable continuous changeover between grid-connected and islanded modes, provide resilience against grid disturbances, and enhance sustainability of energy **(Cortes et al., 2017)**. The main parts of MG are: PV systems **(Kumar et al., 2019)**, WT **(Abdulwahab et al., 2022; Jibril et al., 2019; Dreidy et al., 2017; Babatunde et al., 2020)**, and Synchronous DG needed to supplement renewable sources like PV and WTs **(Sen and Bhattacharyya, 2014)**.



2.1 Energy Storage Systems

Energy storage systems such as BESS (Lukman et al., 2020), SUPCAs (Ali et al., 2023; Cabrane et al., 2016; Kamel et al., 2019), and SMES (Li et al., 2017) play a crucial role in MGs (Ali et al., 2023). They help maintain power balance by charging during excess generation and discharging when required. Storage provides frequency regulation, and voltage support, smoothens output of renewables and enhances reliability (Datta et al., 2021).

2.1.1 Modeling of the BESS

Fig. 1 presents an equivalent model of BESS.

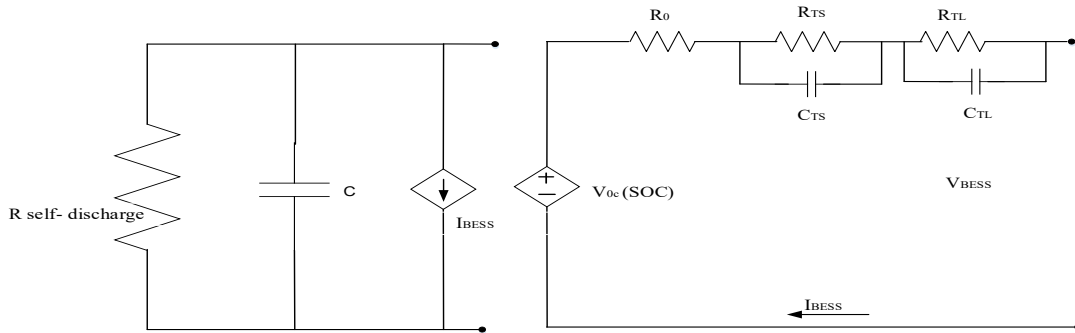


Figure 1. The BESS model

The BESS model includes the BESS voltage and SOC equations. The power output of the BESS is defined by Eq. (1).

$$P_{BESS} = V_{BESS} \times I_{BESS} \tag{1}$$

where, P_{BESS} is the BESS output power, V_{BESS} is the BESS voltage and I_{BESS} is the BESS current.

Thus, the voltage equation for the BESS in the dynamic droop control strategy is given by Eq. (2);

$$V_{BESS} = R_{BESS} \times I_{BESS} + V_{BESS_{SOC}} \tag{2}$$

where, R_{BESS} is the BESS internal resistance and $V_{BESS_{SOC}}$ is the additional voltage component related SOC of the BESS.

The capacity model produces energy quantity C_{BESS} that the BESS could restore based on mean discharging current. Corresponding expressions are established starting from I_{MD} current, as compared to operation mode C_{MD} in which ΔT represent accumulated heating as shown in Eq. (3) (Cabrane et.al, 2016).

$$\frac{C_{BESS}}{C_{MD}} = \frac{1.67}{1 + 0.67 \left(\frac{I_{BESS}}{I_{MD}} \right)^{0.9}} \times (1 + 0.005\Delta T) \tag{3}$$

The SOC is represented by Eq. (4) which is derived from Eq. (3):



$$\frac{dSOC_{BESS}}{dt} = \frac{1}{C_{BESS}} \times (P_{IN_{BESS}} - P_{BESS}) \tag{4}$$

where, SOC_{BESS} is the BESS SOC, $P_{IN_{BESS}}$ is the BESS power input and P_{BESS} is the BESS power output

2.1.2 Control Systems

Advanced hierarchical control systems are required to maintain voltage, frequency stability and ensure proper load sharing between DERs in the MG (Ali et al., 2023). Droop control, virtual impedance methods, and power management schemes are implemented through fast local controllers.

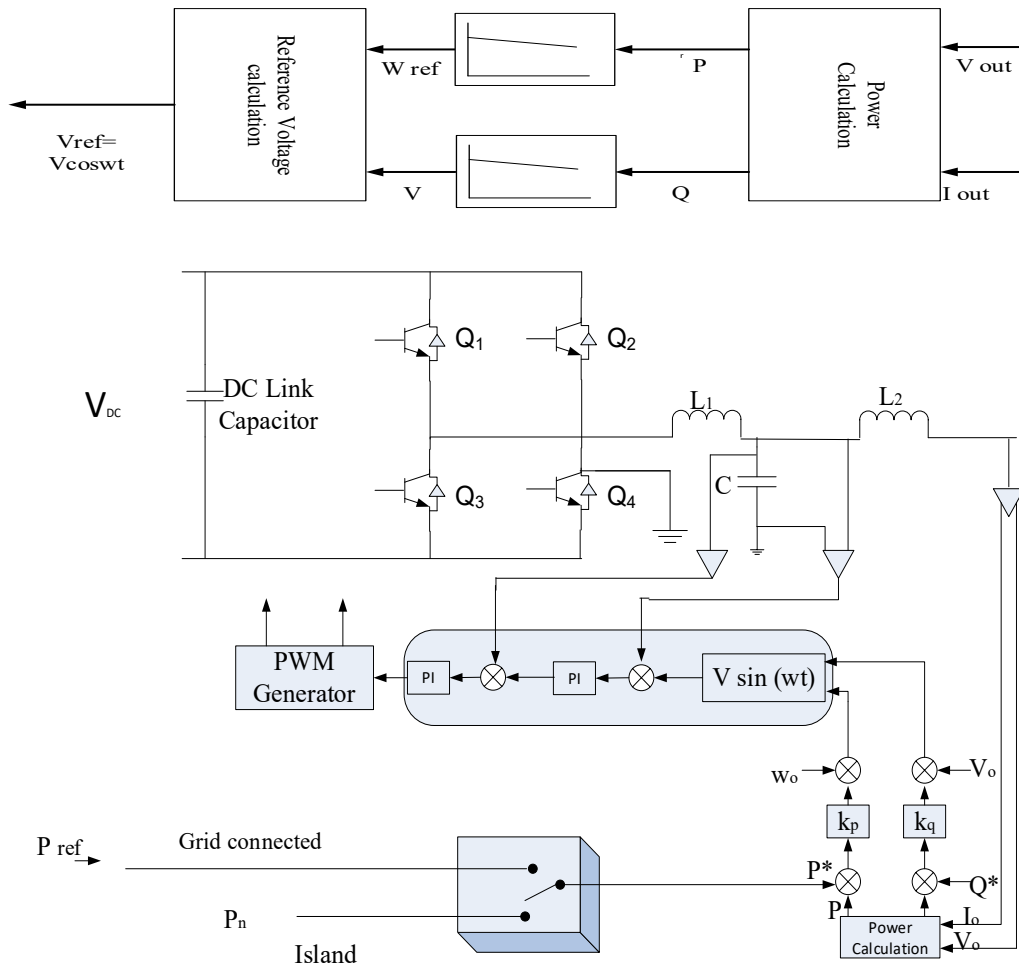


Figure 2. PQ-Model of 3-Phase Inverter

The DC-bus voltage is control based on principle shown in Fig. 2. PI corrector evaluates reference current I_{dcref} needed to sustain DC-bus voltage at referred voltage V_{ref} . An EMS delivers reference currents for static-converters $I_{BESS ref}$ BESS, SUPCA $I_{SUPCA ref}$ and SMES $I_{SMES ref}$. These currents make sure that voltage for DC-bus is fixed not minding the load attitude and the value of power removed from hybrid connected systems whose operation is a factor of Droop loop. When any issue arises on any BESS, SUPCA or SMES ensure that DC-



bus voltage is regulated. At all times, the sum of all referred currents, $I_{BESS\ ref}$, $I_{SUPCA\ ref}$ and $I_{SMES\ ref}$, must be equal to I_{dcref} using Eq. (5) which is modified version of the model in the work of (Cabrane et al., 2016).

$$I_{dcref} = I_{BESS\ ref} + I_{SUPCA\ ref} + I_{SMES\ ref} \quad (5)$$

The DC-bus voltage could be modeled using Eq. (6);

$$C_{dc} \frac{dv_{dc}}{dt} = i_{P\ dc} + i_{BESS\ dc} + i_{SUPCA\ dc} + i_{SMES\ dc} - i_{Load} \quad (6)$$

In Eq. (6), $I_{P\ dc}$, $I_{BESS\ dc}$, $I_{SUPCA\ dc}$ and $I_{SMES\ dc}$, represent the DC current of DERs, BESS, SUPCA and SMES respectively, I_{Load} represents load current. C_{dc} represents the capacity of central bus which would allow impressive voltage for DC-bus to load and other index Current control system provide reference for stored current for DC-bus. This signal moves by low passage to BESS, SMES or SUPCA BESS current which is in exponential form.

2.1.3 Power Balance and Load Demand Analysis

The power balance in the islanded MG is governed by output power as shown in Eq. (7). It provides the correlation between the power output of the DG, wind turbine, and PV systems within the MG.

$$P_{MG} = P_{DG} + P_{WT} + P_{PV} + P_{BESS} + P_{SMES} + P_{SUPCA} - P_{Load} - P_{Loss} \quad (7)$$

In Eq. (7), P_{MG} represents the total power output of the MG, P_{Load} represents total power consumed by the load within the MG, P_{Loss} represents any power losses within the MG. The system losses are approximated as Eq. (8):

$$P_{Loss} = k \times P_{MG} \quad (8)$$

where, k is the loss factor. Losses include transmission, converter and other load flow losses. For this work, the losses are about 3% of total output power. The relationship between power and current for any element is given by Eq. (9):

$$P = V \times I \quad (9)$$

where, P is power, V is voltage, and I is current. This applies to all generators, storage systems, and loads.

By coordinating the BESS, SUPCA, and SMES, the HESS optimally balances steady-state and dynamic power requirements. The HESS is interfaced to the AC MG through a PQ 3-phase inverter, shown in Fig. 2. The proposed HESS MG model is shown in Fig. 3.

To ensure that the power generated by Fig. 3 is continuously adjusting to the load, and variation in this balance which can cause frequency alteration in the system, this current study proposes Dynamic V-F Droop Controller that is exhibited in section 3.2.

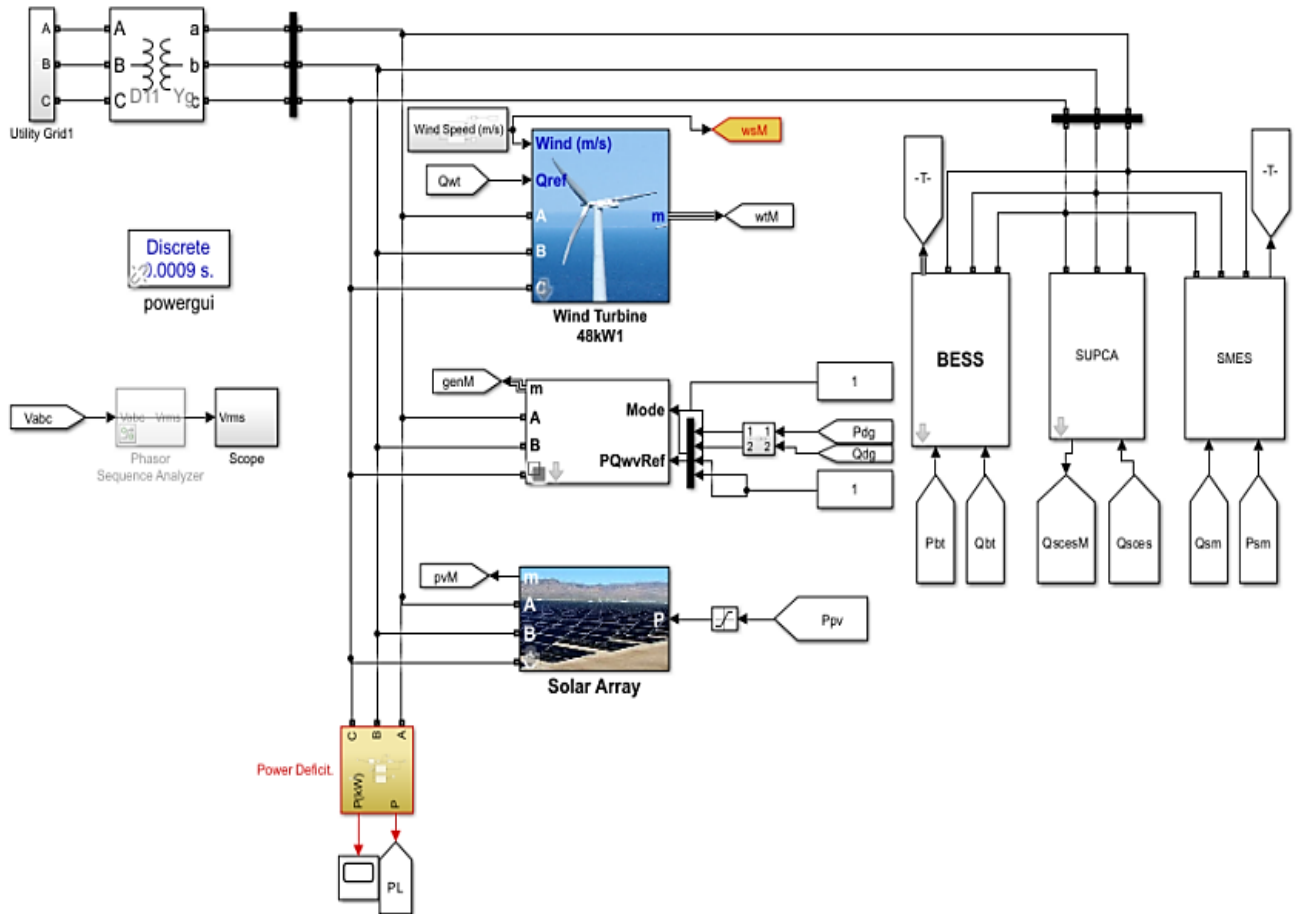


Figure 3. The Proposed HESS MG Model

2.2 Conventional Droop Control Method

Droop controls are de-concentrated comparative power apportioning technique mostly adopted in power control and load allocation for inverter-based DERs in MGs (Opiyo, 2018). It permits DERs to allocate power demand proportionately, based on their ratings less the need for any external linkage (Cortes et al., 2017). Each DER is given a particular droop feature that specifies the connections between its power output and departure in voltage and frequency. A droop feature is modeled as slope or droop coefficient. Based on its droop feature, a DER adjusts its output power in response to the alteration in voltage and frequency. A DER with positive droop characteristic would reduce its power output with rise in voltage or frequency; while a DER with negative droop attribute, would increase its power output. This adjustment is crucial in restoring voltage or frequency to their nominal level. Droop control technique gives DERs chance to respond to alterations in load in decentralized way without needing for central control. It encourages load apportioning between DERs, and also, sustains stability for MG. In grid-connected MGs, additional control mechanisms are employed to comply with grid regulations and maintain synchronization with the main grid. The conventional droop control approach has certain limitations that need to be addressed. These limitations include load sharing accuracy being affected by line impedances between DERs, which can result in poor active and reactive power sharing. Additionally, differences in feeder impedances can degrade the sharing of harmonics between inverters. Large transient droop during sudden load changes or islanding can cause frequency and voltage



deviations. Furthermore, there may be steady-state errors in maintaining the desired nominal values of frequency and voltage. Stability issues can arise due to active power-voltage coupling at high R/X ratio and low system damping. Another limitation is the occurrence of circulating currents among parallel inverters due to the lack of synchronization.

3. PROPOSED ENHANCED DROOP CONTROL

3.2 Dynamic Droop Gain Control Strategy

The conventional droop control is enhanced by using dynamic droop gains instead of fixed gains. The proposed control scheme implements two dynamic droop controllers - one for voltage control and one for frequency control.

3.2.1 Dynamic Voltage Control

Voltage droop control starts with the voltage reference and adds the voltage droop component which adjusts the MG voltage based on the frequency deviation from the reference. Then, it subtracts the voltage droop components related to the BESS, SMES, and SUPCA currents as given by Eq. (10) which is an improved equation from (Li et al., 2016). These components account for voltage droop brought about by the current flowing through each energy storage component of the HESS.

$$V_{mg} = V_{ref} + Droop_V \times (f_{mg} - f_{ref}) - Droop_{V_{BESS}} \times I_{BESS} - Droop_{V_{SMES}} \times I_{SMES} - Droop_{V_{SUPCA}} \times I_{SUPCA} \quad (10)$$

In Eq. (10), V_{mg} denotes MG voltage, V_{ref} is the voltage reference, $Droop_V$ is the voltage droop coefficient, f_{mg} is the MG frequency, f_{ref} is the frequency reference, $Droop_{V_{BESS}}$ is the voltage droop factor for BESS, $Droop_{V_{SMES}}$ is voltage droop factor for SMES and $Droop_{V_{SUPCA}}$ represents voltage droop factor for SUPCA.

3.2.2 Dynamic Frequency Control

Dynamic Frequency Control starts with frequency reference and adds the frequency droop component which quickly adjusts the MG frequency according to the power variation from the reference. It then adds the frequency droop components related to currents of the SMES ($Droop_{V_{SMES}} \times I_{SMES}$), and SUPCA ($Droop_{V_{SUPCA}} \times I_{SUPCA}$). The droop components in the hybrid system account for the frequency droop brought about by the current passing through each energy storage component. The MG frequency droop control is expressed by Eq. (11) improved from (Li et al., 2016).

$$f_{MG} = f_{ref} + Droop_f \times (P_{MG} - P_{ref}) - Droop_{f_{BESS}} \times I_{BESS} - Droop_{f_{SMES}} \times I_{SMES} - Droop_{f_{SUPCA}} \times I_{SUPCA} \quad (11)$$

In Eq. (11), P_{MG} is the MG power, P_{ref} is the MG power reference, $Droop_f$ is the frequency droop coefficient, $Droop_{f_{BESS}}$ represents frequency droop factor for BESS, $Droop_{f_{SMES}}$ is

frequency droop factor for SMES and $Droop_{f_{SUPCA}}$ represent frequency droop factor for SUPCA.

Fig. 4 shows the proposed dynamic droop V-F controller. This is developed using Eqs. (10 and 11). The produced power must continually align with load, and fluctuation or alteration in this balance could trigger frequency alteration in this system. In normal and conventional power system, short time power misalignment is mostly covered using kinetic energy from power generators known as main frequency control. Modeling the Primary Frequency-Control (PFC) system is carried out using Eq. (12) improved from (Li et al., 2016); and shown in **Fig. 4**.

$$\frac{df}{dt} = \frac{f_0}{2 \sum H_i} \left(\sum P_{G_i} - \sum P_{L_i} \right) + D_{SMES} \Delta P_{SMES} + D_{BESS} \Delta P_{BESS} + D_{SUPCA} \Delta P_{SUPCA} \quad (12)$$

In Eq. (12), the D_{SMES} , D_{BESS} and D_{SUPCA} are the droop coefficients of the SMES, BESS and SUPCA systems respectively. The system voltage is also able to be maintained by regulating the reactive power using the SMES, BESS, and the SUPCA hybrid energy storage.

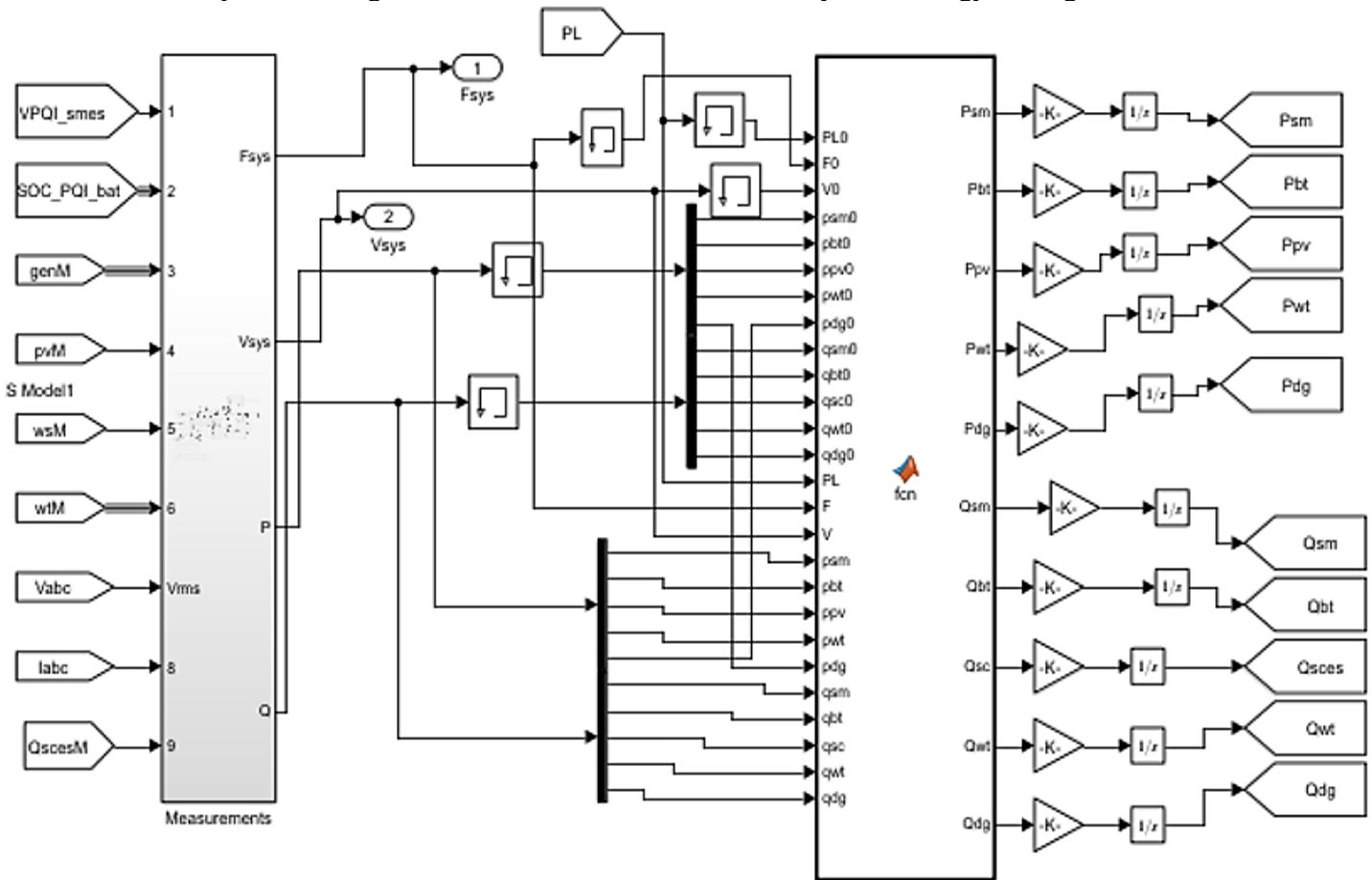


Figure 4. MATLAB SIMULINK Diagram of Proposed Dynamic V-F Droop Controller

Since D_{SMES} , D_{SUPCA} and D_{BESS} represent droop indexes for SMES, SUPCA and BESS arrangement respectively. The voltage of this system could be maintained and sustained by controlling reactive power with SMES, SUPCA and BESS. **Fig. 5** presents the block diagram



for reactive power control. Based on the reactive power discrepancy, ΔQ creates Voltage error for the system and the error is analyzed by controller and then returned as the referenced reactive component V_{q_ref} . Then, V_{q_ref} will be employed in generating PWM signals needed to control the SMES/SUPCA/BESS compensation reactive power.

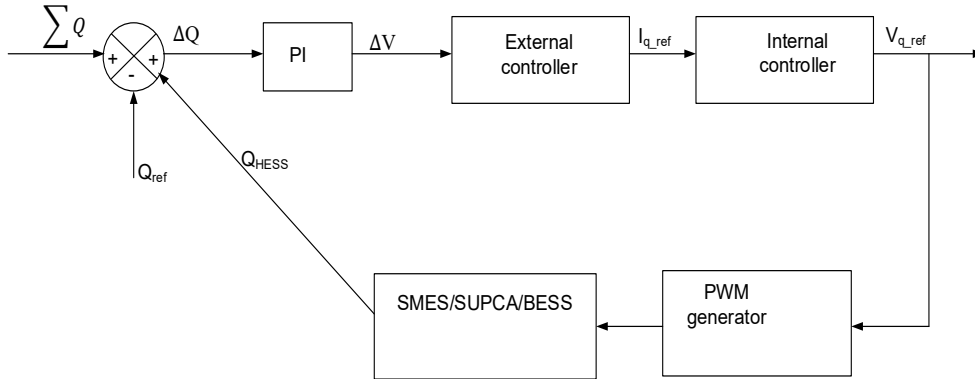


Figure 5. Block diagram of Reactive Power Regulation using SMES/SUPCA/BESS as a HESS.

3.3 The Controlled Mechanism of the Modified HESS

Fig. 6 is a modification of that used by (Li et al., 2017). But at this time, SUPCA was introduced in the control system. Control technique represented in Fig. 6 is accomplished in two sections, AC-end voltage control and DC-end droop control. Based on this schematic, HESS is arranged as voltage source to recompense for system change and variation. Three DC/DC converters were utilized to cover this battery, SUPCA and SMES in DC-bus, so that their droop features could be designed.

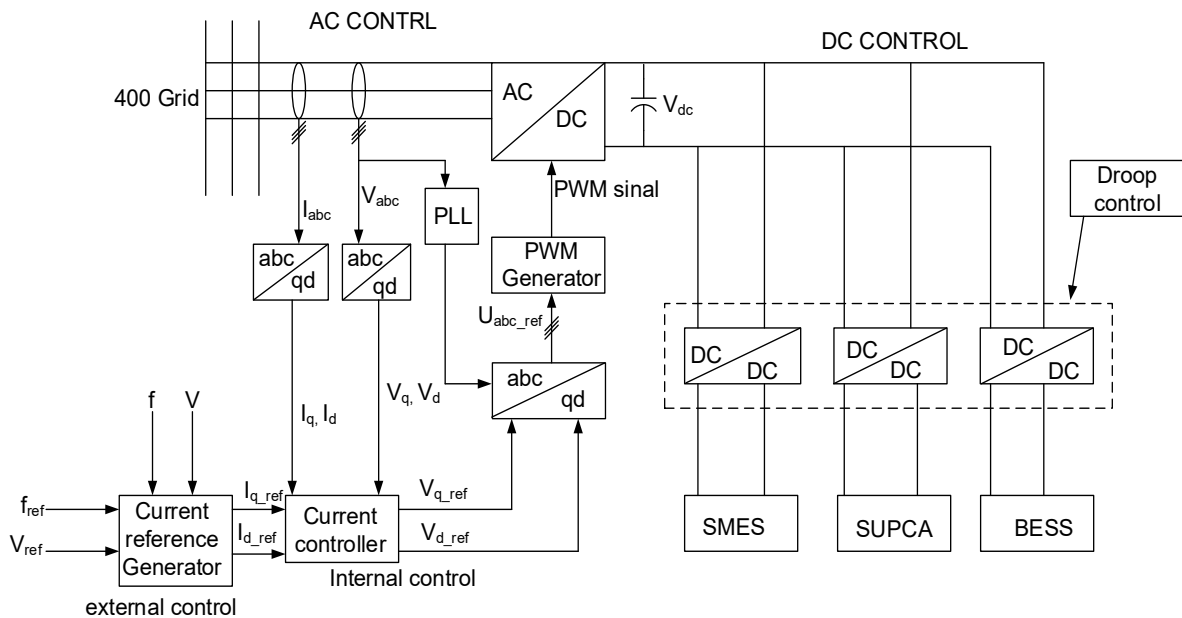


Figure 6. Control system for proposed MG along with HESS.



3.4 Proposed SECANT Dynamic Droop Control Algorithm

The active and reactive power are controlled using the proposed SECANT dynamic droop control algorithm. The algorithm dynamically predicts the active and reactive set-point for each of the generating and storage resources. The algorithm also ensures and improved system stability via a dynamic droop sensitive factor. The dynamic droop control (DDC) algorithm is developed using a discrete approach that employs the SECANT fixed-point iteration numerical approximation method (**Hasija et.al, 2023**). The algorithm uses a set of present and past, active and reactive power set-points ($P_{g,ref}(k)$ and $Q_{g,ref}(k)$) to estimate the future power generation schedule ($P_{g,ref}(k+1)$ and $Q_{g,ref}(k+1)$) of the generating/storage resource (GS). The pseudocode for the proposed DDC algorithm is represented in **Fig. 7**. In the approach, once the present and past measurements of active and reactive power are measured, together with the respective microgrid frequency and voltage. The microgrid p.u frequency deviations can be estimated using Eq. (13).

$$df(k+1) = \begin{cases} 1 - \frac{f(k-1)dP_{net}(k) - f(k)dP_{net}(k-1)}{(dP_{net}(k) - dP_{net}(k-1))f_n} & |dP_{net}(k) - dP_{net}(k-1)| > 0 \\ 0 & |dP_{net}(k) - dP_{net}(k-1)| = 0 \end{cases} \quad (13)$$

$$dP_{net}(k) = P_L(k) - \sum_{g \in GS} P_{g,ref}(k) \quad (14)$$

where $df(k+1)$ represents the future normalized frequency deviation estimate of the microgrid, k represents the index of sample, f and f_n represent the microgrid actual and nominal operating frequency vectors respectively, dP_{net} represents the total active power deviation vector of the microgrid, P_L represents the total network active load. Whereas, the microgrid p.u voltage deviations can be estimated using Eq. (15).

$$dv(k+1) = \begin{cases} 1 - \frac{v(k-1)dQ_{net}(k) - v(k)dQ_{net}(k-1)}{(dQ_{net}(k) - dQ_{net}(k-1))v_n} & |dQ_{net}(k) - dQ_{net}(k-1)| > 0 \\ 0 & |dQ_{net}(k) - dQ_{net}(k-1)| = 0 \end{cases} \quad (15)$$

$$dQ_{net}(k) = Q_L(k) - \sum_{g \in GS} Q_{g,ref}(k) \quad (16)$$

where $dv(k+1)$ represents the future normalized voltage deviation estimate of the microgrid, k represents the index of sample, v and v_n represents microgrid actual and nominal operating voltage vectors respectively, dQ_{net} represents the total reactive power deviation vector of the microgrid. Q_L represents the total network reactive load.

Additionally, the total active and reactive power deviations can be estimated using Eqs. (17) and (18) respectively.

$$dp(k+1) = \begin{cases} df(k+1) \frac{dP_{net}(k)}{f_n - f(k)} & |f_n - f(k)| > 0 \\ 0 & |f_n - f(k)| = 0 \end{cases} \quad (17)$$

And:



$$dq(k+1) = \begin{cases} dv(k+1) \frac{dQ_{net}(k)}{v_n - v(k)} & |v_n - v(k)| > 0 \\ 0 & |v_n - v(k)| = 0 \end{cases} \quad (18)$$

where $dp(k+1)$ and $dq(k+1)$ represents the future active and reactive power deviation estimates of the microgrid respectively. To ensure improved performance, active and reactive power droop sensitivity factors ($Kp_{g,DSF}$ and $Kq_{g,DSF}$) are designed using Eqs. (19) and (20) for each of the generating/storage resource, to minimize the system's voltage and frequency settling time.

$$Kp_{g,DSF} = \begin{cases} \frac{|df(k+1)|}{|(P_{g,ref}(k) - P_{g,ref}(k-1) - P_L(k) + P_L(k-1))|} & |(P_{g,ref}(k) - P_{g,ref}(k-1) - P_L(k) + P_L(k-1))| > 0 \\ 1 & |(P_{g,ref}(k) - P_{g,ref}(k-1) - P_L(k) + P_L(k-1))| = 0 \end{cases} \quad (19)$$

Similarly:

$$Kq_{g,DSF} = \begin{cases} \frac{|dv(k+1)|}{|(Q_{g,ref}(k) - Q_{g,ref}(k-1) - Q_L(k) + Q_L(k-1))|} & |(Q_{g,ref}(k) - Q_{g,ref}(k-1) - Q_L(k) + Q_L(k-1))| > 0 \\ 1 & |(Q_{g,ref}(k) - Q_{g,ref}(k-1) - Q_L(k) + Q_L(k-1))| = 0 \end{cases} \quad (20)$$

Lastly, the future active and reactive power schedule of each generating/storage unit can be estimated using Eqs. (21) and (22) respectively.

$$P_{g,ref}(k+1) = \begin{cases} P_{g,ref}(k) - \alpha_{g,p} \frac{dp \cdot Kp_{g,DSF}}{Kp_{g,DSF} + \sum_{i \in GS, i \neq g} Kp_{i,DSF}} & f(k) > f_n \quad \& \quad P_{g,ref}(k) > P_{g,min} \\ P_{g,min} & f(k) > f_n \quad \& \quad P_{g,ref}(k) = P_{g,min} \\ P_{g,ref}(k) + \alpha_{g,p} \frac{dp \cdot Kp_{g,DSF}}{Kp_{g,DSF} + \sum_{i \in GS, i \neq g} Kp_{i,DSF}} & f(k) < f_n \quad \& \quad P_{g,ref}(k) < P_{g,max} \\ P_{g,max} & f(k) < f_n \quad \& \quad P_{g,ref}(k) = P_{g,max} \end{cases} \quad (21)$$

Also:

$$Q_{g,ref}(k+1) = \begin{cases} Q_{g,ref}(k) - \alpha_{g,q} \frac{dq \cdot Kq_{g,DSF}}{Kq_{g,DSF} + \sum_{i \in GS, i \neq g} Kq_{i,DSF}} & v(k) > v_n \quad \& \quad Q_{g,ref}(k) > Q_{g,min} \\ Q_{g,min} & v(k) > v_n \quad \& \quad Q_{g,ref}(k) = Q_{g,min} \\ Q_{g,ref}(k) + \alpha_{g,q} \frac{dq \cdot Kq_{g,DSF}}{Kq_{g,DSF} + \sum_{i \in GS, i \neq g} Kq_{i,DSF}} & v(k) < v_n \quad \& \quad Q_{g,ref}(k) < Q_{g,max} \\ Q_{g,max} & v(k) < v_n \quad \& \quad Q_{g,ref}(k) = Q_{g,max} \end{cases} \quad (22)$$



Finally, the future power generation schedule ($P_{g,ref}(k+1)$ and $Q_{g,ref}(k+1)$) of the generating/storage, serves as the reference set-point for next simulation time step. The parameters $\alpha_{g,p}$ and $\alpha_{g,q}$ are the constant active and reactive power dynamic droop coefficients which can be optimally determined using any meta-heuristic optimization technique. However, in this paper, their value was selected to be 1p.u. In general, the proposed SECANT dynamic droop control algorithm is presented in **Fig. 7**.

1. Input: $f, f_n, v, v_n, P_L, Q_L, P_{g,ref}, Q_{g,ref}, \alpha_{g,p}, \alpha_{g,q}$, and GS
2. Read $f(k-1), P_L(k-1), P_{g,ref}(k-1)$
3. Evaluate $f(k), P_L(k), P_{g,ref}(k)$
4. Evaluate the total active power deviations $dP_{net}(k)$ and $dP_{net}(k-1)$ using Eq. (14)
5. Forecast the next frequency deviation $df(k+1)$ using Eq. (13)
6. Forecast the next total active power deviation $dp(k+1)$ using Eq. (17)
7. For $g \in GS$
8. Forecast the active power dynamic droop sensitivity $Kq_{g,DSF}$ using Eq. (20)
9. Forecast the next active power schedule $P_{g,ref}(k+1)$ Eq. (21)
10. End
11. Evaluate $v(k), Q_L(k), Q_{g,ref}(k)$
12. Evaluate $v(k-1), Q_L(k-1), Q_{g,ref}(k-1)$
13. Evaluate the total reactive power deviations $dQ_{net}(k)$ and $dQ_{net}(k-1)$ using Eq. (16)
14. Forecast the next voltage deviation $dv(k+1)$ using Eq. (15)
15. Forecast the next total reactive power deviation $dq(k+1)$ using Eq. (18)
16. For all $g \in GS$
17. Evaluate the reactive power dynamic droop sensitivity $Kq_{g,DSF}$ using Eq. (20)
18. Forecast the next reactive power schedule $Q_{g,ref}(k+1)$ using Eq. (22)
19. End
20. Output: $P_{g,ref}(k+1), Q_{g,ref}(k+1)$ for all $g \in GS$

Figure 7. SCANT Dynamic Droop Control Algorithm

3.5 The Flow Chart of the Designed MATLAB/Simulink Model

Fig. 8 is a flow chart for a microgrid system arrangement in MATLAB/SIMULINK, which will generate Power $\sum PG$ and $\sum QG$. The generated P and Q are used to control the voltage and frequency of this designed model, respectively. In the constant droop gain (CDG) method, an initial value is assigned, while the dynamic droop gain (DDG) control is set to 1 for both frequency and voltage control processes.

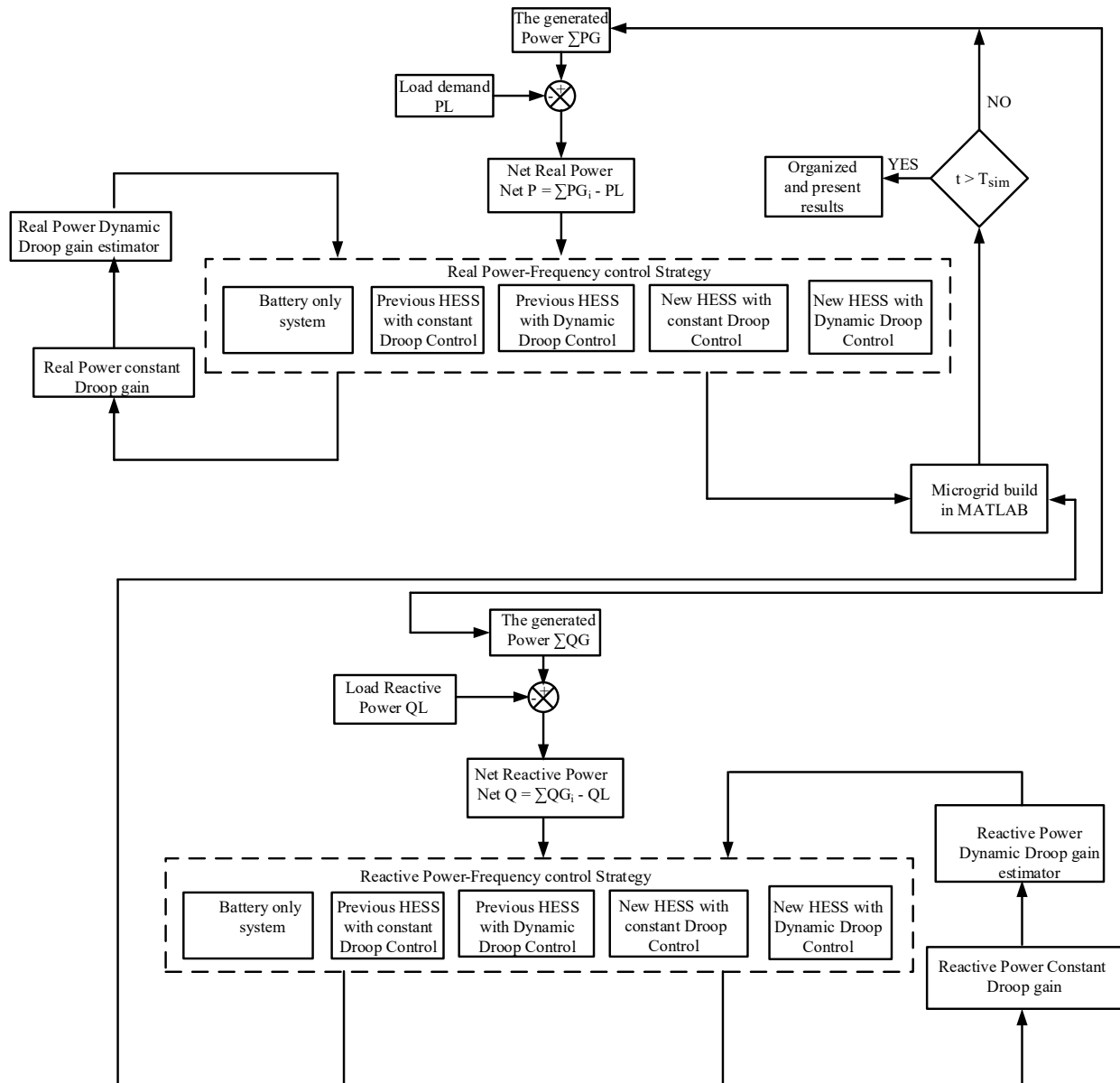


Figure 8. Flow chart of the proposed microgrid system

4. RESULTS AND DISCUSSION

In order to study and validate the effects of the proposed enhanced Dynamic Droop Control for MG Frequency and Voltage Stabilization, the load profile that was used in (Li et al., 2016) was adopted and presented in Fig. 9. The proposed scheme is validated using the parameters in Appendix A.

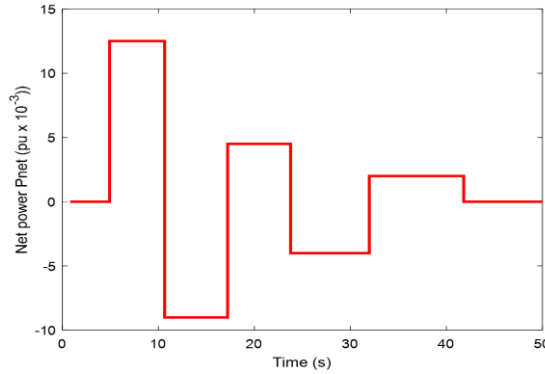


Figure 9. Random Load Changes

4.1 BESS State of Charge

This subsection of the paper presents detailed results from simulation studies examining five cases to demonstrate the effectiveness of the proposed enhanced droop control strategy using hybrid energy storage to improve BESS SOC in the MG system. The five cases are:

Case 1 - Microgrid with only BESS

When only BESS is used for energy storage without any droop control, the charging/discharging current fluctuates significantly around 40 A peak as seen in Fig. 10. The BESS must supply the entire dynamic current demand leading to high oscillations. The BESS SOC varies widely between 5 % to 92 % as shown in Fig. 11. This indicates excessive BESS cycling that reduces lifespan. The Total Harmonic Distortion (THD) is very high around 303 % as observed in Fig. 12.

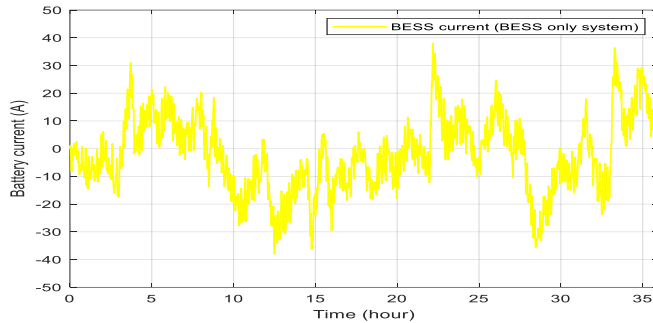


Figure 10. BESS current changes with time.

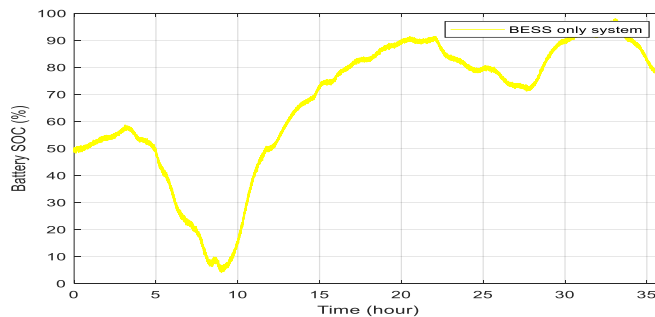


Figure 11. BESS SOC variation with time.

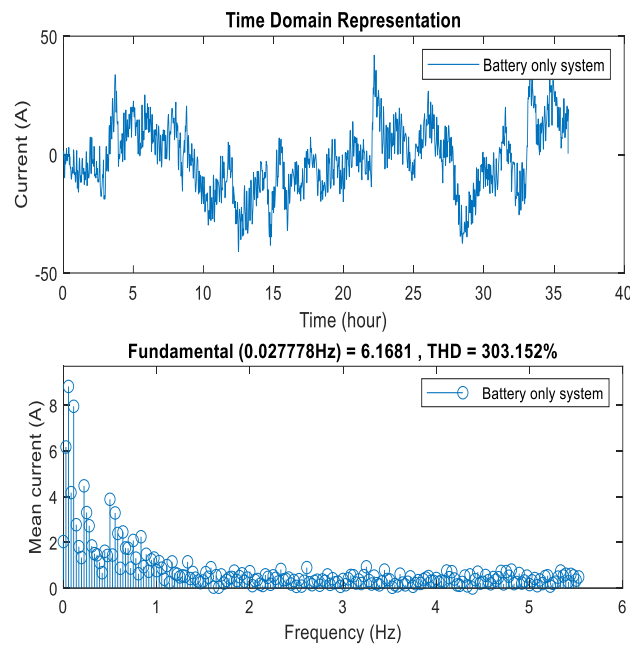


Figure 12. Harmonic on BESS only system

Case 2 - Microgrid with BESS and SMES Using Constant Droop Gains

Implementing constant droop control for BESS and SMES reduces current fluctuations compared to Case 1 as seen in **Fig. 13**. The SOC range improves to 25-82 % in **Fig. 14** demonstrating the benefit of coordinated BESS and SMES control. However, the harmonics are still significant with THD of 290 % in **Fig. 15** due to lack of proper correction.

Case 3 - Microgrid with BESS and SMES using Dynamic Droop Gains

The scenario with dynamic droop gain for BESS and SMES demonstrated even better performance. Adopting dynamic droop gains further smoothens the current profile as shown in **Fig. 16** compared to Case 2.

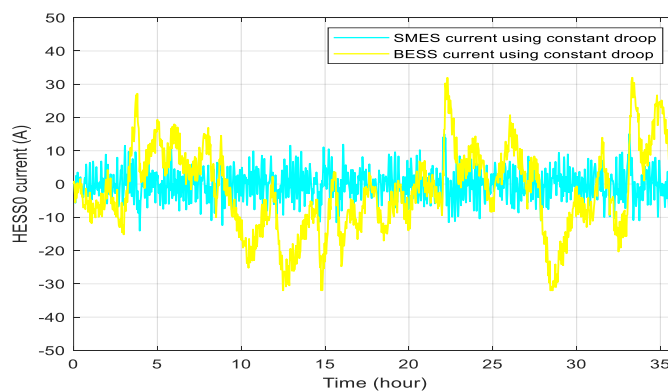


Figure 13. Current variation with respect to time in BESS and SMES using constant droop gain.

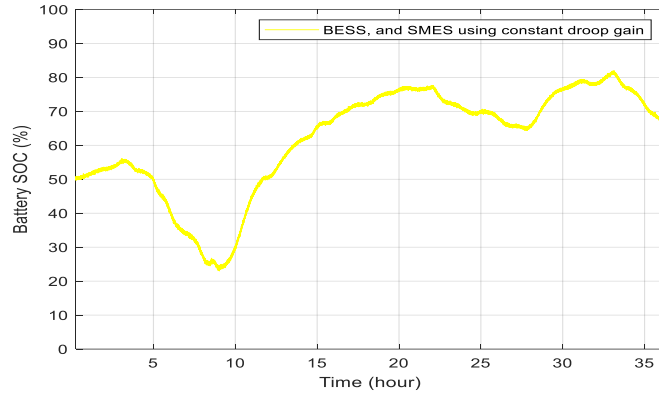


Figure 14. SOC variation with respect time on BESS and SMES using constant droop gain.

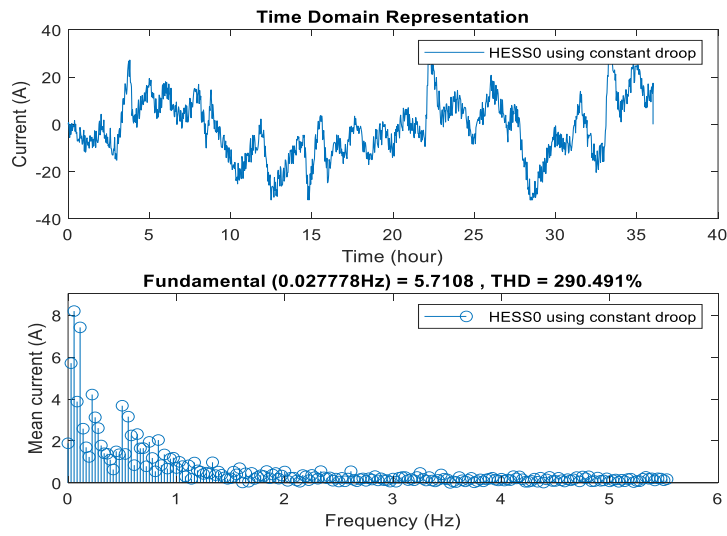


Figure 15. Harmonic on BESS and SMES using constant droop gain.

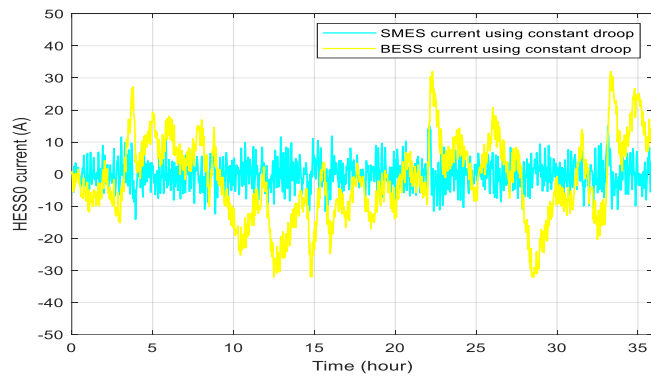


Figure 16. Current variation with time on BESS and SMES using Dynamic Droop gain.



The SOC range in **Fig. 17** increases slightly to 28-80 % as the optimization of dynamic gains reduces BESS cycling. But the harmonics in **Fig. 18** are still undesirably high around 289 % THD.

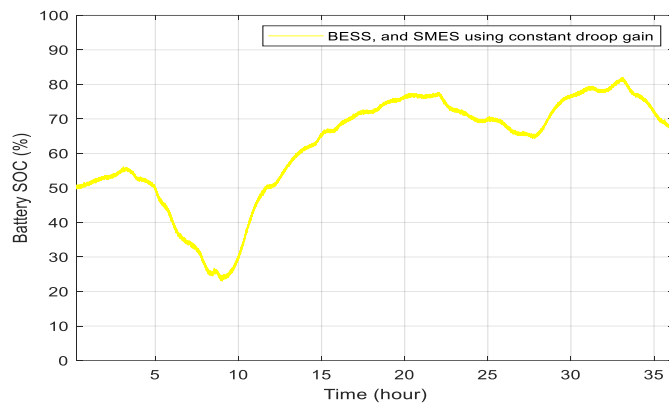


Figure 17. SOC variation with time on BESS and SMES using constant droop gain.

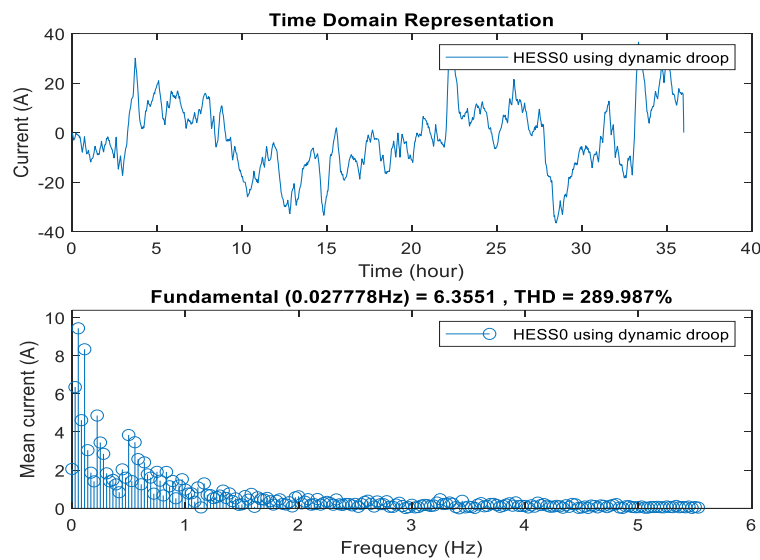


Figure 18. Harmonic on BESS and SMES using Dynamic Droop gain

Case 4 - Microgrid with BESS, SMES and SUPCA using Constant Droop Gains
 Adding a SUPCA to the HESS configuration improves results compared to Cases 1-3. The currents in **Fig. 19** are more stable. The SOC operation range expands notably to 29-72 % in **Fig. 20** due to SUPCA handling power fluctuations. The THD also reduces to 287 % in **Fig. 21** as the SUPCA provides reactive power support.

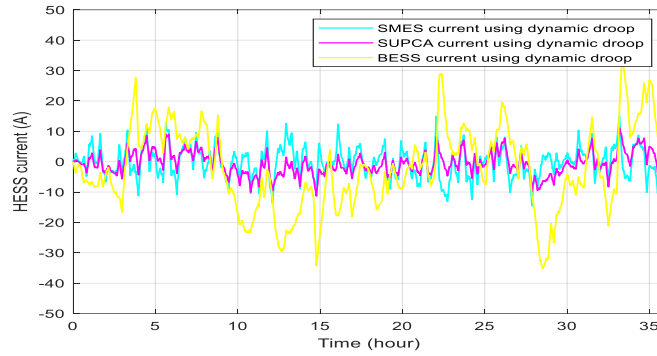


Figure 19. SOC variation with time on BESS, SMES and SUPCA using Constant Droop gain.

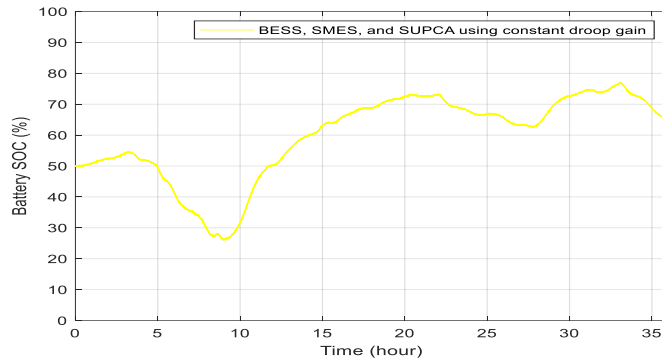


Figure 20. SOC variation with time on BESS, SMES and SUPCA using Constant Droop gain.

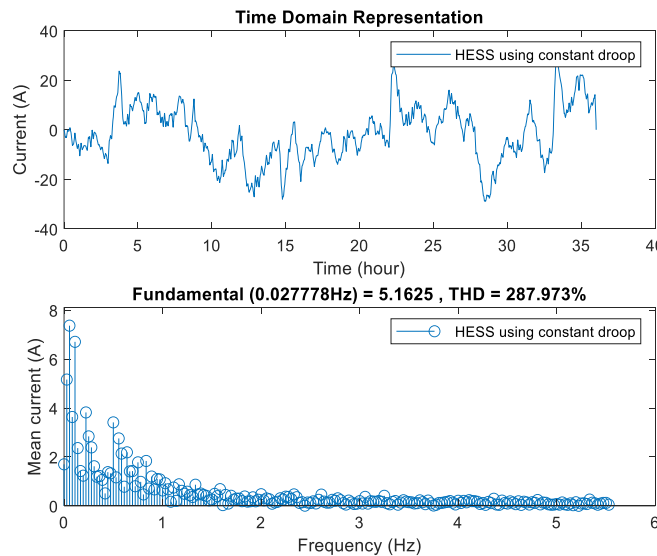


Figure 21. Harmonic on BESS, SMES and SUPCA using Constant Droop gain

Case 5 - Microgrid with BESS, SMES and SUPCA using Dynamic Droop Gains

Further improvements are achieved by using dynamic gains for the SUPCA-enhanced HESS system. The SOC is tightly regulated between 48-74 % in **Fig. 23** owing to the optimized coordination of BESS, SMES and SUPCA. The current profile in **Fig. 22** is smooth with no distortions while the THD reduces by 277 % as seen in **Fig. 24**.

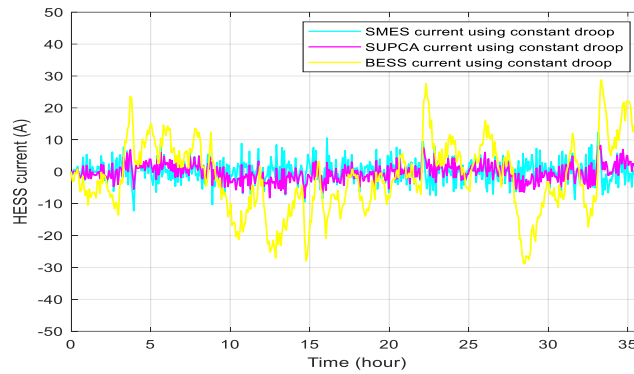


Figure 22. SOC variation with respect to time on BESS, SMES and SUPCA using Dynamic Droop gain.

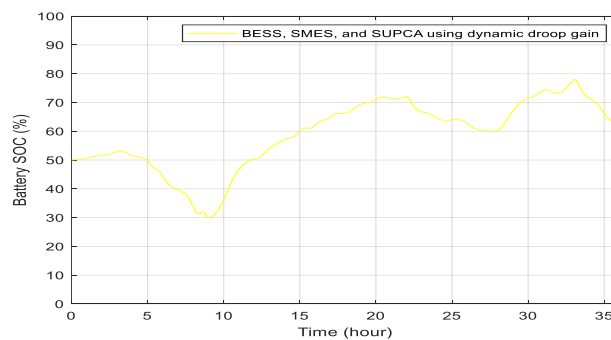


Figure 23. SOC variation with respect to time on BESS, SMES and SUPCA using Dynamic Droop gain

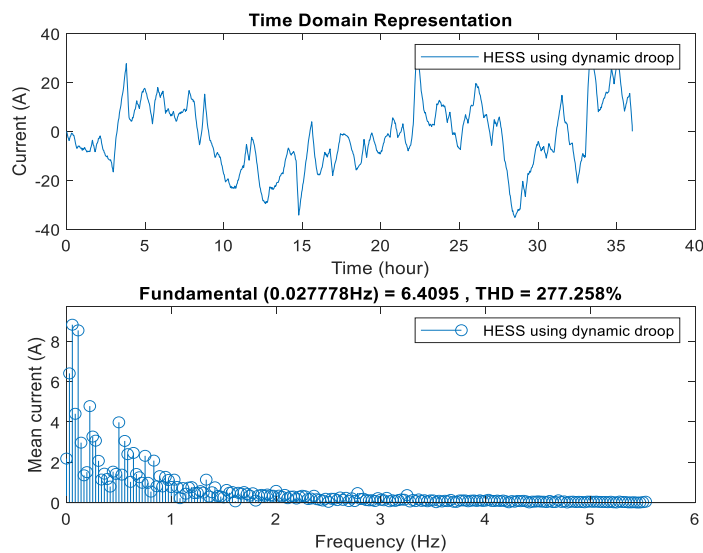


Figure 24. Harmonic on BESS, SMES and SUPCA using Dynamic Droop gain

4.2 Frequency and Voltage Control

The impact of the proposed SUPCA/SMES/BESS for frequency and voltage control in the MG system is shown in **Figs. 25 and 26.**

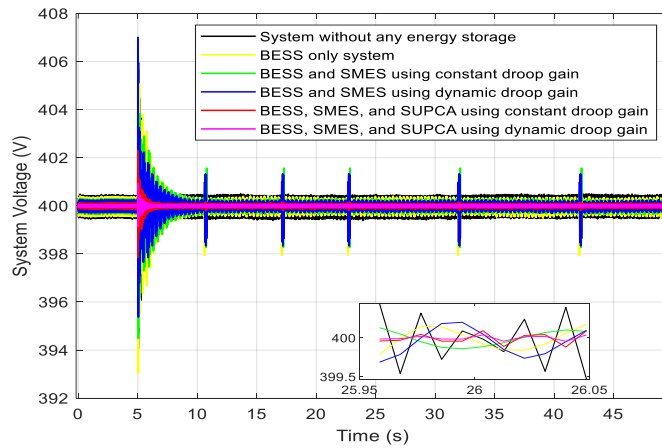


Figure 25. Voltage variations the five cases

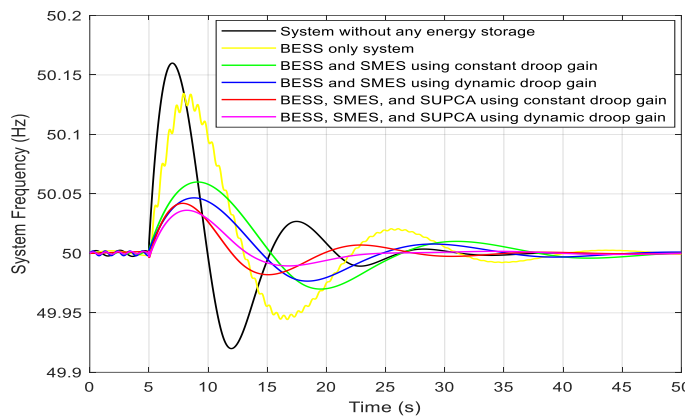
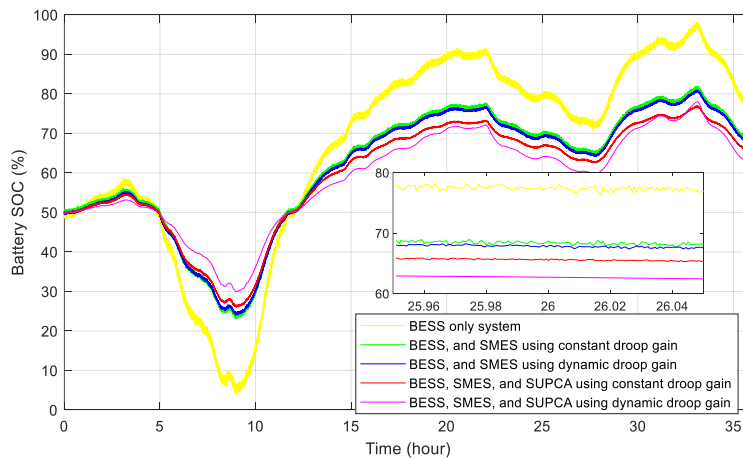


Figure 26. Frequency oscillations in the five cases.

The impact on BESS state of charge (SOC) profile across the five cases is presented in Fig. 27.

Figure 27. State of Charge in the five cases



The results demonstrate that integrating SUPCA in the HESS configuration and leveraging an enhanced dynamic droop control strategy significantly improves the PFC, voltage regulation and SOC compared to conventional approaches. The proposed technique harnessing the strengths of each storage element provides superior performance in maintaining power



system stability under varying generation and load conditions. The key findings from this research are summarized as follows:

1. The mathematical modeling of the MG components including generators, HESSs, and droop controllers was successfully implemented in MATLAB/Simulink.
2. The introduction of a SUPCA in the hybrid storage configuration along with BESS and SMES improved the overall system performance compared to using batteries or SMES alone.
3. The proposed enhanced dynamic droop control strategy optimized using the SECANT method provided superior voltage and frequency stabilization compared to conventional fixed droop gains.
4. The coordination of different hybrid storage elements and optimized dynamic gains extended the BESS lifetime by reducing charge/discharge cycles.
5. Power quality was enhanced with lower total harmonic distortion using the proposed control approach.
6. Faster transient response and steady-state setpoint regulation were achieved using the online optimized dynamic droop gains.
7. The SUPCA further improved the transient performance by mitigating power fluctuations through rapid charging/discharging.

Thus, the integrated control and storage solution effectively addressed key MG stability challenges under varying renewable generation.

5. CONCLUSIONS

This paper has presented a unique control strategy for MGs by integrating dynamic droop control optimization with a HESS comprising BESS, SUPCA, and SMES. The DDGs are tuned in active-time using the rapid-converging SECANT numerical method to provide enhanced stability under varying conditions. The hybrid storage combines the steady power supply capacity of BESS with the transient overload handling capability of SUPCA.

Comprehensive simulation studies demonstrate that the proposed approach significantly enhances the voltage and frequency regulation, power sharing accuracy, BESS lifespan, and overall control performance compared to conventional droop methods. The SUPCA further improves the system response by mitigating power fluctuations. This research enables the effective utilization of renewable energy and distributed generators in resilient MG networks by leveraging advanced control techniques and emerging storage technologies. While the developed control strategy showed significant improvements, further studies can be undertaken:

1. The impact of the proposed approach under different configurations, renewable penetration levels, and load profiles can be evaluated.
2. Additional studies under grid-connected mode and transition between grid-connected/islanded modes could be performed.
3. Higher harmonic currents are still present in the system, and as such future researchers can consider the development of an active power filters to further minimize the harmonic current in the system.



NOMENCLATURE

Symbol	Description	Symbol	Description
$P-f$	Power factor	$Droop_f$	Frequency droop coefficient
ΔT	Temperature gradient	$df(k+1)$	Future normalized frequency deviation
C_{BESS}	Capacity model	k	Index of sample
P_{Loss}	Power loss	f and f_n	Microgrid actual and nominal operating frequency vectors
ρ	loss factor	$dv(k+1)$	Future normalized voltage deviation
$Droop_v$	voltage droop coefficient	dQ_{net}	Total reactive power deviation vector
f_{ref}	frequency reference	K	Droop sensitivity factors

Acknowledgements

The authors are thankful for the resources rendered by the Tertiary Education Trust Fund (TETFUND), Petroleum Technology Development Fund (PTDF), and Department of Electrical & Electronics Engineering, Faculty of Engineering, University of Lagos, Lagos, Nigeria; which substantially helped this study.

Credit Authorship Contribution Statement

K.U. Udeze: Writing–original draft, review & editing, Validation, Methodology, and Data collection. S.O. Adetona: Writing–review & editing, Validation, Methodology, and Data collection

Declaration of Competing Interest

The authors declare that they have no known competing financial interests or personal relationships that could have appeared to influence the work reported in this paper

REFERENCES

- Abdulwahab, I., Abubakar, A. S., Olaniyan, A., Sadiq, B. O., and Faskari, S. A., 2022. *Control of Dual Stator Induction Generator Based Wind Energy Conversion System*. IEEE Nigeria 4th International Conference on Disruptive Technologies for Sustainable Development (NIGERCON), pp. 1-5. <https://doi.org/10.1109/NIGERCON54645.2022.9803100>
- Aghamohammadi, M. R., and Abdolahinia, H., 2014. Electrical Power and Energy Systems A new approach for optimal sizing of battery energy storage system for primary frequency control of islanded Microgrid. *International Journal Of Electrical Power And Energy Systems*, 5(4), pp. 325–333. <https://doi.org/10.1016/j.ijepes.2013.07.005>
- Ali, Z. M., Calasan, M., Aleem, S. H. E. A., Jurado, F., and Gandoman, F. H., 2023. Applications of Energy Storage Systems in Enhancing Energy Management and Access in Microgrids: A Review. *Energies*, 16(16), p. 5930, <https://doi.org/10.3390/en16165930>
- Babatunde, O. M., Munda, J., and Hamam, Y., 2020. A Comprehensive State-of-the-Art Survey on Hybrid Renewable Energy System Operations and Planning. *IEEE Access*, 8, pp. 75313–75346, <https://doi.org/10.1109/ACCESS.2020.2988397>
- Budi, A.L.S., Anam, S., Ashari, M. and Soeprijanto, A., 2020, December. Energy management control based on standalone photovoltaic battery and supercapacitor hybrid energy storage system using PI controller. In *International Seminar of Science and Applied Technology (ISSAT 2020)* (pp. 1-7). Atlantis Press. <https://doi.org/10.2991/aer.k.201221.001>



- Cabrane, Z., Ouassaid, M., and Maaroufi, M., 2016. Analysis and evaluation of battery-supercapacitor hybrid energy storage system for photovoltaic installation. *International Journal of Hydrogen Energy*, pp. 1–11. <https://doi.org/10.1016/j.ijhydene.2016.06.141>
- Cortes, C. A., Contreras, S. F., and Shahidehpour, M., 2017. Microgrid Topology Planning for Enhancing the Reliability of Active Distribution Networks. 3053(c), in *IEEE Transactions on Smart Grid*. 9(6), pp. 6369-6377. <https://doi.org/10.1109/TSG.2017.2709699>
- Datta, U., Kalam, A., and Shi, J., 2021. A review of key functionalities of battery energy storage system in renewable energy integrated power systems. *Energy Storage*, 3(5), e224, <https://doi.org/10.1002/est2.224>
- Dreidy, M., Mokhlis, H., and Mekhilef, S., 2017. Inertia response and frequency control techniques for renewable energy sources: A review. *Renewable and Sustainable Energy Reviews*, 69(5), pp. 144–155. <https://doi.org/10.1016/j.rser.2016.11.170>
- Fu, Q., Nasiri, A., Solanki, A., Bani-Ahmed, A., Weber, L., and Bhavaraju, V., 2015. Microgrids: architectures, controls, protection, and demonstration. *Electric Power Components and Systems*, 43(12), pp. 1453–1465, <https://doi.org/10.1080/15325008.2015.1039098>
- Hajiaghahi, S., Salemnia, A., and Hamzeh, M., 2019. Hybrid energy storage system for microgrids applications: A review. *Journal of Energy Storage*, 21(11), pp. 543–570. <https://doi.org/10.1016/j.est.2018.12.017>
- Hasija, T., Ramkumar, K. R., Singh, B., Kaur, A., and Mittal, S. K., 2023. A new Polynomial based Symmetric Key Algorithm using Polynomial Interpolation Methods. *2023 IEEE 12th International Conference on Communication Systems and Network Technologies (CSNT)*, pp. 675–681
- Ibrahim, A., Jibril, Y., and Haruna, Y. A. S., 2017. Determination of Optimal Droop Controller Parameters for an Islanded Microgrid System Using Artificial Fish Swarm Algorithm. *International Journal of Scientific & Engineering Research*, 8(3), pp. 959-965,
- Jibril, Y., Olarinoye, G., Abubakar, A., Abdulwahab, I., and Ajayi, O., 2019. Control Methods Used in Wind Energy Conversion System: A Review. *ATBU Journal of Science, Technology and Education*, 7(2), pp. 53-59.
- Kamel, A., Rezk, H., Shehata, N., Thomas, J., 2019. Energy management of a DC microgrid composed of photovoltaic/fuel cell/battery/supercapacitor systems. *Batteries*, 5(3), P. 63; <https://doi.org/10.3390/batteries5030063>
- Kim, Y., Kim, E., and Moon, S., 2016. *Frequency and Voltage Control Strategy of Standalone Microgrids with High Penetration of Intermittent Renewable Generation Systems*. 31(1), pp. 1-11, <https://doi.org/10.1109/TPWRS.2015.2407392>.
- Kumar, M., Morla, S. K., and Mahanty, R. N., 2019. Modeling and simulation of a Micro-grid connected with PV solar cell & its protection strategy. *2019 4th International Conference on Recent Trends on Electronics, Information, Communication & Technology (RTEICT)*, pp. 146–150. <https://doi.org/10.1109/RTEICT46194.2019.9016924>.
- Li, J., Xiong, R., Yang, Q., Liang, F., Zhang, M., and Yuan, W. , 2017. Design/test of a hybrid energy storage system for primary frequency control using a dynamic droop method in an isolated microgrid power system. *Applied Energy*, 20(1), pp. 257–269. <https://doi.org/10.1016/j.apenergy.2016.10.066>
- Lin, X., and Lei, Y., 2017. Coordinated Control Strategies for SMES-Battery Hybrid Energy Storage Systems. *IEEE Access*, 5, pp. 23452–23465. <https://doi.org/10.1109/ACCESS.2017.2761889>
- Marzebali, M. H., Mazidi, M., and Mohiti, M., 2020. An adaptive droop-based control strategy for fuel



cell-battery hybrid energy storage system to support primary frequency in stand-alone microgrids. *Journal of Energy Storage*, pp. 101-127. <https://doi.org/10.1016/j.est.2019.101127>

Oguntosin, V., and Ogbechie, P. T., 2023. Advances in Electrical Engineering, Electronics and Energy Design and construction of a foam-based piezoelectric energy harvester. *E-Prime - Advances in Electrical Engineering, Electronics and Energy*, 4(5), pp. 100-175. <https://doi.org/10.1016/j.prime.2023.100239>

Opiyo, N. N., 2018. Droop Control Methods for PV-Based Mini Grids with Different Line Resistances and Impedances. *Scientific Research Publishing*, 9, pp. 101-112. <https://doi.org/10.4236/sgre.2018.96007>

Ren, Y., Rind, S. J., and Jiang, L., 2020. A coordinated control strategy for battery/supercapacitor hybrid energy storage system to eliminate unbalanced voltage in a standalone AC microgrid. *Journal of Intelligent Manufacturing and Special Equipment*, 1(1), pp. 3-23. <https://doi.org/10.1108/jimse-08-2020-0007>

Saeed, M. H., Fangzong, W., Kalwar, B. A., Iqbal, S., and Member, S., 2021. A Review on Microgrids' Challenges & Perspectives. *IEEE Access*, 9, pp. 166502-166517. <https://doi.org/10.1109/ACCESS.2021.3135083>

Sen, R., and Bhattacharyya, S. C., 2014. Off-grid electricity generation with renewable energy technologies in India: An application of HOMER. *Renewable Energy*, 6(2), pp. 388-398. <https://doi.org/10.1016/j.renene.2013.07.028>

Serban, I., and Marinescu, C., 2014. Electrical Power and Energy Systems Battery energy storage system for frequency support in microgrids and with enhanced control features for uninterruptible supply of local loads. *International Journal of Electrical Power and Energy Systems*, 5(4), pp. 432-441. <https://doi.org/10.1016/j.ijepes.2013.07.004>

Appendix

The system simulation parameter		
MG generator parameters		
	Diesel generator output power	100 kw
	Wind turbine output power	48 kw
	Solar PV output power	17 kw
BESS parameters		
	Type	60 Ah lead acid
	Voltage	12 V
	Matrix size	4 x 20
	Bank terminal voltage	4 x 12
	Max. discharging current	30 A
	Power rating	10 kW
	Max energy	100 kW h
The SUPCA parameters		
	Reactive Power	10 KVAR
	Time Constant (τ)	1×10^{-4} sec
The SMES Subsystem ratings		
	Rated power	10 kW
	Inductance	1.4 H
	Standard current	150 A
	Critical current	250 A
	Energy capacity	20.23 kJ
	Highest power	202.3 kW

تحكم ديناميكي محسن في التدد الشبكة الصغيرة وثبيت الجهد باستخدام أنظمة تخزين الطاقة الهجينة: نهج طريقة SECANT

ساندي اوديبي، كينيث اديتونا*

قسم الهندسة الكهربائية والإلكترونية، جامعة لاغوس، لاغوس، نيجيريا.

خلاصة

نظرًا لطبيعتها المتغيرة والمتقطعة، فإن تكامل مصادر الطاقة المتجددة يطرح تحديات تحكم تتعلق باستقرار الجهد والتردد في الشبكات الصغيرة المعزولة. تقترح هذه الورقة استراتيجية محسنة للتحكم الديناميكي في التدد تم تحسينها في الزمن الفعال جنبًا إلى جنب مع نظام تخزين الطاقة الهجين (HESS) الذي يشتمل على نظام تخزين طاقة البطارية (BESS) والمكثفات الفائقة (SUPCA) وتخزين الطاقة المغناطيسية فائقة التوصيل (SMES) لتحسين استقرار الشبكة الصغيرة. يتم ضبط مكاسب التدد الديناميكي (DDG) بشكل مستمر باستخدام الطريقة العددية SECANT سريعة التقارب لتعزيز الاستجابة العابرة وأداء الحالة المستقرة، وقد تم تحقيق ذلك باستخدام MATLAB/Simulink. يجمع HESS بين الخصائص التكميلية لـ BESS و SUPCA و SMES لتحقيق التوازن بين إمدادات الطاقة الثابتة وقدرة التحميل الزائد المؤقتة. تتحقق دراسات المحاكاة التفصيلية على نظام اختبار الشبكة الصغيرة من أن استراتيجية التحكم المقترحة تعزز بشكل كبير تنظيم الجهد/التردد، ودقة مشاركة الطاقة، وفترة عمل BESS والاستقرار العام مقارنة بتقنيات التدد التقليدية. تعمل SUPCA أيضًا على تحسين الأداء العابر وجودة الطاقة من خلال تخفيف التقلبات. يوضح البحث طريقة مبتكرة لاستغلال خوارزميات التحكم المتقدمة وتقنيات التخزين الناشئة للجيل القادم من الشبكات الصغيرة المرنة والمستدامة.

الكلمات المفتاحية: الشبكة الصغيرة، أنظمة تخزين الطاقة، تخزين طاقة البطارية، تخزين الطاقة المغناطيسية فائقة التوصيل، المكثفات الفائقة.